nature ecology & evolution

SUPPLEMENTARY INFORMATION

https://doi.org/10.1038/s41559-019-1092-y

In the format provided by the authors and unedited.

The consequences of craniofacial integration for the adaptive radiations of Darwin's finches and Hawaiian honeycreepers

Guillermo Navalón[1,2,3]*, Jesús Marugán-Lobón[2,4], Jen A. Bright[5], Christopher R. Cooney[6] and Emily J. Rayfield[1]*

[1]School of Earth Sciences, University of Bristol, Bristol, UK. [2]Unidad de Paleontología, Departamento de Biología, Universidad Autónoma de Madrid, Madrid, Spain. [3]Department of Earth Sciences, University of Oxford, Oxford, UK. [4]Dinosaur Institute, Natural History Museum of Los Angeles County, Los Angeles, CA, USA. [5]Department of Biological and Marine Sciences, University of Hull, Hull, UK. [6]Department of Animal and Plant Sciences, University of Sheffield, Sheffield, UK. *e-mail: guillermo.navalon@earth.ox.ac.uk; e.rayfield@bristol.ac.uk

Supplementary Information for:

The consequences of craniofacial integration on the adaptive radiations of Darwin's finches and Hawaiian honeycreepers

Guillermo Navalón, Jesús Marugán-Lobón, Jen A. Bright, Christopher R. Cooney & Emily J. Rayfield

Extended Results

Detailed patterns and rates of craniofacial evolution in landbirds

Whole skull

The three first principal components (PCs) account for 75.94 % of the total shape variation of the superimposed complete skull landmark configurations (Fig. 2; Extended Data Fig. 2). PC1 explains 43.7 % of the total shape variance and describes differences in proportions (i.e., the relative size of beak to the rest of the skull), coupled with changes in beak shape (including nares, landmarks 5 and 6; Extended Data Fig. 1 and Extended Data Table 1, for landmark, block and region definitions) but only very subtle shape changes in the cranium. Positive scores are associated with long straight beaks (landmarks 1-4 and semilandmarks 19-23; e.g., *Ramphastos*, Piciformes*; Tockus,* Bucerotiformes; *Falculea,* Passeriformes) and negative scores with short curved beaks with slightly more rounded nares (e.g. *Micropsitta,* Psittaciformes; *Geospiza,* Passeriformes; *Harpagus,* Accipitriformes). As General Procrustes Analysis superimposition (GPA) spreads variation across the total configuration (SI. Fig. 4) it is ambiguous whether the differences in proportions described by PC1 (but also the other axes) represent evolutionary changes in the relative size of the beak only, the rest of the skull, or both regions at the same time. Hence, thereafter differences in proportions and arrangement angles will be described as changes in the beak size and shape with respect to the rest of the skull.

PC2 explains 24.34% of shape variation and describes both changes in relative proportions and shapes of beak and skull (Fig. 2; Extended Data Fig. 2). Positive scores are associated with thin, chisel-like beaks, with narrow, anterioposteriorly expanded nares, slightly smaller beaks than crania, and skulls with straight lacrimal-ecthethmoid regions (landmarks 12 and 13), flat palate regions (landmarks 7 and 8), and small quadrates (landmarks 9-11; e.g, *Xenicus,* Passeriformes; *Todus,* Coraciiformes). Negative scores are associated with long, curved beaks, with rounded, posteriorly protracted nares, an anteriorly expanded braincase (landmarks 14-17), posterioventrally extended lacrimal-ecthethmoid region, inclined palate, and larger quadrates (e.g., *Buceros,* Bucerotiformes; *Vestiaria,* Passeriformes).

Taxa are not evenly distributed in the morphospace, and the plot of PC1 and PC2 separates the major radiations of landbirds into three clusters (Fig. 2; Extended Data Fig. 2). The first is located in the negative quarter of both axes and encompasses all parrots (Psittaciformes) and a handful of disparate passerines (Passeriformes, e.g., *Geospiza magnirostris*). The second cluster is located in the negative region of PC2 but in the positive extreme of PC1, and comprises all hoopoes, woodhoopoes, and hornbills (Bucerotiformes), true toucans (Ramphastidae, Piciformes), and some passerines (e.g., *Epimachus, Falculea, Vestiaria*). The last cluster is spread along the whole PC1 axis but is mostly restricted to scores between -0.10 and 0.10 in PC2 and includes all other taxa. Passerines (Passeriformes) are spread along the whole cluster, with highest density in the region delimited by 0.05-0.10 in PC1 and 0-0.1 in PC2. The latter region is also shared with many representatives of Coraciiformes (kingfishers, rollers, bee-eaters, and kin), Piciformes (toucanets, barbets, woodpeckers, and kin), Trogoniformes (trogons), and Cariamiformes (serimas). Strigiformes (owls and barn owls), Accipitriformes (hawks, eagles, vultures, and kin), Falconiformes (falcons and caracaras), Coliiformes (mousebirds), Leptosomatiformes (cuckoo-roller), and

Opisthocontiformes (hoatzin) largely overlap in the negative PC1 region of the third cluster, with a scatter of species of passerines (e.g., *Paradoxornis, Pseudonestor, Geospiza conirostris*). Longirostrine coraciiforms (e.g., *Merops*) and piciforms (e.g., *Galbula*) occupy the positive PC1 region of this cluster shared with some other longirostrine passerine taxa (e.g., *Xiphorhynchus*).

Finally, PC3 explains only 4.86% of total shape variation, and describes coupled differences in both the beak and skull without apparent changes in proportions (Fig. 2; Extended Data Fig. 2). Positive scores are associated with thin, straight beaks with anterioposteriorly extended narrow nares, larger neurocrania, inclined palate regions, and a posterioventrally expanded lacrimal-ecthethmoid region. Negative scores are associated with curved beaks with more rounded nares, smaller neurocrania, flat, posteriorly displaced palate regions, and a straight lacrimal-ecthethmoid region. This axis nicely separates the two (non-sister) groups of diurnal raptors (Falconiformes and Accipitriformes, which have extreme negative scores) from the rest of the lineages of landbirds. Some owls (e.g., *Bubo*), parrots (e.g., *Cacatua*), and the toucan barbet (e.g., *Semnornis ramphastinus,* Extended Data Fig. 1) are recovered close to the diurnal raptors.

Rates of evolution for the whole skull are heterogeneous, as expected (Cooney et al. 2017, Felice and Goswami, 2018), although not to the degree that Felice & Goswami (2018) recovered (Fig. 2; Extended Data Fig. 2; SI. Table 1). Discrepancies are likely due to differences in landmark data, but also a higher number of taxa for each landbird lineage in our study that buffers abrupt morphological change between higher clades (i.e. order-parvorder level), reconstructing main patterns of craniofacial evolution with higher fidelity.

Faster evolving clades include most notably Hawaiian honeycreepers and Darwin's finches which show the highest sustained rates among the whole landbird radiation and to a lesser degree, Old World vultures (Aegypiinae and Gypaetinae), exhibiting several rate shifts associated with further increased rate of evolution in terminals of both (Fig. 2; Extended Data Fig. 2; SI. Table 1). Fast bursts of evolution also occur in the branch leading to clades with very extreme craniofacial anatomy such as true toucans (Ramphastidae) or hoopoes, woodhoopoes and hornbills (Bucerotiformes), and individual disparate terminal taxa like extreme longirostrine passerines (e.g. *Falculea palliata,* Vangidae; *Epimachus fastuosus,* Paradiseidae; *Rupicula peruvianus,* Cotingidae; *Arachnothera magna,* Nectariniidae) or non-passerines with divergent morphologies with respect to their parent clades (e.g., the pigmy parrot, *Micropsitta finschii*; the laughing kookaburra, *Dacelo novaeguineae*). Moderate bursts of evolution are identified by Variable Rates Analyses (VRAs), for instance, at the node of all ovenbirds (Furnariidae), a well-known continental adaptive radiation[1,2], the node formed by Viduidae, Estrildidae and Ploceidae and the node formed by the divergent snail (*Rosthramus sociabilis*) and plumbeous kites (*Ictinia plumbea*).

Beak block

The first three PCs account for 85.40% of the beak shape variance (Fig. 2; Extended Data Fig. 2; SI. Table 2). PC1 explains 51.23% of the total shape variance and describes differences in depth and curvature, coupled with differences in the shape and position of the nares. This major axis describes very similar beak shape changes to those of previous studies[1,3]. Positive scores are associated with thin, straight beaks with narrow anteriodorsally extended

nares (e.g., *Myiagra, Phylidomiris*), whereas negative scores are associated with deep, curved beaks with rounded, posteriorly-restricted nares (e.g. *Cacatua*). PC1 therefore separates Strigiformes, Accipitriformes, Falconiformes, Psittaciformes, and a scatter of unrelated deep-beaked passerines (e.g., *Paradoxornis*) from the rest of the lineages. PC2 explains 27.03% of beak shape variance and describes differences in depth, curvature, and position and shape of nares. Negative scores are associated with deep, tapering beaks with only a slight curvature in the tip and anterioposteriorly extended narrow nares (e.g., *Ninox*). Positive scores are associated with slightly thinner, curved beaks with posteriorly restricted rounded nares (e.g., *Bucorvus*). Most lineages are restricted to a narrow central area in these axes. Divergent taxa include longirostrine passerines (e.g. *Epimachus*) and non-passerines (e.g., *Upupa*), and a rather compact isolated cluster including the hornbills (Bucerotidae: Bucerotiformes) and true toucans (Ramphastidae: Piciformes). PC3 explains only 7.14% of the total beak shape variance and describes minor differences in beak shape and more acute differences in nares shape. Positive scores are associated with deep, tapering beak that are curved towards the tip, with narrow extended nares, whereas negative scores are associated with deep, curved beaks with posteriorly-restricted, rounder nares. Most of the landbird radiation is restricted to slightly positive scores. The only outlier in the positive side of PC3 is the cuckoo roller (*Leptosomus discolor*). Negative scores are typical of most Falconiformes and the toucan barbet (*Semnornis ramphastinus*). Some passerines (e.g. *Rupicola, Pityriasis*) also exhibit extreme negative scores.

VRAs inferred a rate shift affecting the most recent common ancestor (MRCA) of Ramphastidae (true toucans) and its sister *Semnornis ramphastinus* (Fig. 2; Extended Data Fig. 3; SI. Table 3). Other moderate increase in beak shape evolution include the branch leading to Falconiformes, the MRCA of an assemblage of families within Corvides, and the MRCA of Ploceidae, Estrildidae, and Viduidae, within the Passerida. As with the whole skull configuration, beak shape evolution in both Darwin's finches and Hawaiian honeycreepersis characterized by higher rates than the rest of landbirds, including individual rate shifts in both HH and DF.

Skull block

The first three PCs account for only 70.41% of skull shape variance, indicating shape change in the skull block is spread over more shape dimensions than shape change in the beak block or the whole skull configurations (Fig. 2; Extended Data Fig. 4). PC1 accounts for 38.38% of total skull shape variation, and positive scores along this axis are associated with skulls with small neurocrania, dorsoventrally-shortened, straight lacrimal-ecthethmoid regions, horizontal palate regions, and small quadrates (e.g., *Lophaetus,* Accipitriformes; *Baryphthengus,* Coraciiformes). Negative scores are associated with anteriorly-expanded, large neurocrania, posterioventrally-expanded lacrimal-ecthethmoid regions, tilted palates, and large quadrates (*Ara,* Psittaciformes; *Pseudonestor,* Passeriformes). This axis separates parrots (Psittaciformes) with extreme negative scores from all other landbirds. Some diverging individual taxa from other lineages bridge the gap between parrots and the rest (e.g., *Pseudonestor,* Passeriformes; *Psilopogon,* Piciformes; *Athene,* Strigiformes) as well as complete families like the woodpeckers (e.g., *Sphyrapicus, Picus*; Picidae, Piciformes).

PC2 accounts for 22.22% of the total skull shape variation and is associated with differences in the position of lacrimal-ecthecthmoid and palate regions, and changes in the relative size of the neurocranium and quadrates. Positive scores are associated with skulls with posteroventrally oriented lacrimal-ecthethmoid regions, flat palate regions, small quadrates, and large neurocrania (e.g., *Certhia, Xenicus*). Negative scores are associated with tilted palate regions, larger quadrates, and smaller neurocrania (e.g., *Selenidera*; Piciformes). Main radiations of landbirds largely overlap in this axis of shape variation, with some slight regionalization. For instance, passerines largely occupy the positive region of this axis with only some outliers exploring more negative values (e.g., *Pseudonestor*, *Geospiza magnirostris*), whereas Accipitriformes are more restricted to the negative region. There is some regionalization within major orders with different families diverging to different areas. For instance, within Piciformes, toucans (Ramphastidae), toucan-barbets (Semnornithidae), and barbets (Lyiibidae, Megalaimidae and Capitonidae) scatter in the negative region while woodpeckers (Picidae) occupy the positive region.

PC3 explains 9.82% of the total skull shape variance. Positive scores are associated with skulls with dorsoventrally shortened and posterioventrally tilted lacrimal-ecthethmoid regions and anteriorly displaced palatines with long pterygoids (palate region; e.g., *Megaceryle,* Coraciiformes; *Pharomachrus*, Trogoniformes). Negative scores are associated with larger, straight lacrimal-ecthethmoid regions, relatively larger braincases, posteriorly displaced palatines, and short pterygoids (e.g., *Bubo,* Strigiformes). Most landbird lineages cluster around zero on this axis, with some outliers in both the negative (e.g., Falconiformes, Strigiformes) and positive regions (e.g., *Grallaria,* Passeriformes; *Psilopogon,* Piciformes; *Pharomachrus,* Trogoniformes; *Megaceryle,* Coraciiformes).

Skull shape rates are fairly stable across the whole landbird radiation and only few rate shifts affected complete clades and the rest only affect fast evolving terminal taxa. Both Darwin's finches and Hawaiian honeycreepersare characterized by the highest rates of skull shape evolution across both whole families and rate shifts affected the nodes of both clades and the daughter node of Drepanididae defined by *Loxop coccineus* and *Pseudonestor xanthophrys.* An increase towards faster evolution happened in the branch leading to all modern parrots, underlining the fast attainment of their divergent skull anatomy. Remarkably, a shift towards slower rates of skull shape evolution is inferred in the branch leading to the node of Passeri and relatively slow rates of evolution are maintained through the whole clade with only shifts towards higher levels of skull shape evolution associated with the fast-evolving terminal taxa *Epimachus* (Paradiseidae, Corvides), *Coereba* (Thraupidae), and Darwin's finches and Hawaiian honeycreepers.

The effects of rate heterogeneity in evolutionary covariation

Phylogenetic PLS using the time-tree (situation 1) reveals a high number of extreme outliers in many of the analysed clades (SI. Fig. 2). As the computation of Phylogenetic PLS in geomorph assumes a common Brownian motion evolution model for the whole tree (see Methods), these taxa are not likely to conform to a single-rate BM model and are interpreted as very divergent taxa. These outlier taxa generally display higher rates of morphological evolution than the background rates for landbirds, which in some cases underlie large

morphological evolution and a recent origin, and in some cases only the latter. For instance, a recent origin, but not particularly morphological divergences between the parrots *Loriculus galgulus* and *Loriculus philippensis*, are interpreted also as extreme morphological divergence by P-PLS in situation 1, strongly biasing results to a degree that this divergence creates the covariation structure for Psittaciformes which encompasses more than 50 species in our sample (SI. Fig. 2). Therefore, taxa in situation 1 appear as extreme outliers due to a combination of a recent origin and that some of them have undergone particularly large phenotypic evolution when compared to the rest of the landbird radiation (e.g. Darwin's finches and Hawaiian honeycreepers, Fig. 2; SI. Fig. 2) although discriminating between these two factors seems difficult.

Interestingly, however, the pattern of levels of cranial integration across landbirds, remain relatively unaltered between situation 1 (two blocks, time-tree) and situation 2 (two blocks, rate-scaled tree), although the strength of integration is consistently higher in situation 1 (Fig. 4, SI. Fig. 3, Table 1, Supplementary Data 3). Some differences, though, involve comparatively higher cranial integration in diurnal birds of prey (Falconiformes and Accipitriformes) both of which include faster evolving and recent lineages (Fig. 2, Extended Data Figs. 2-4, Supplementary Data 3). Furthermore, clades with higher levels of cranial integration in situation 1 (Supplementary Data 3) are more significantly different to the rest than in situation 2 (Table 1).

These effects are, however, undesirable when the aim is comparing the covariation structure and strength of cranial integration between high-order clades while still incorporating the very interesting outlier taxa. Our approach here using the rate-scaled phylogeny instead of the time tree for P-PLS (situations 2 and 3, see Methods) can accommodate outlier taxa (Figs. 3 & 4). This methodological adjustment is similar to previous attempts to coerce phylogenetic covariation matrices of shape to a BM model by re-scaling branch lengths, but superior in that it permits the estimation of branch lengths using a more complex model (see Methods). Estimation of the fit of P-PLS residuals to a single rate BM model is frequently used to confirm that the data meets the BM expectations of the analyses after transformation of branch lengths[4], however this model fitting methods have shown to lead to frequent model misspecification[5] even if the data is generated under a BM[6]. Therefore, there is not current available method that can allow checking that data fits the assumptions of BM of P-PLS. However, our correction (VRMA rate-scaled branch lengths) permits the assessment of clade-wide covariation patterns including the outlier taxa (Figs. 3 & 4).

The effects of least squares-derived trait correlation artefacts in evolutionary covariaton

Superimposed whole skull configurations for the 436 specimens using Generalized Resistant Procrustes Superimposition (GPRS[7], resistant fit based superimposition[8]) which can portray better than GPA patterns of local variation (see Methods), revealed that a great deal of the shape variation in our sample is concentrated in the beak region, while the rest of the cranial regions seem less variable in shape under this superimposition procedure (SI. Fig 4). Comparisons with superimposed specimens using full Generalized Procrustes Analyses (GPA, least squares superimposition), however, revealed that while consensus shape is very similar (SI. Fig 4, black dots), the individual specimens (SI. Fig 4, grey dots) exhibit considerably less

shape variation in the beak while variation in the other regions of the whole skull configuration has increased dramatically (SI. Fig 4, most obviously in landmark 15; Extended Data Table 1, *crista nucalis*). Therefore, it seems clear that local variation from the beak region is spread across the whole configuration when GPA is used in our sample (SI. Fig 4).

Furthermore, we confirm recent suggestions that this GPA-induced artefacts seriously overstate integration [9]. When we quantified evolutionary covariation between beak and skull blocks in the whole skull configurations (situation 3, within one configuration, rate-scaled tree), most clades exhibit very strong cranial integration (SI. Figs 5 & 6, Supplementary Data 3) consistently higher than in situation 2 (two blocks, rate-scaled tree) (Figs. 3 & 4, Table 1) and to a degree that might suggest that beak shape could be predicted from skull shape, and vice versa. However, the general pattern of levels of cranial integration across landbird is again, roughly consistent with situation 2. Notable differences include that Psittaciformes exhibit comparatively lower levels of cranial integration in situation 3 than in situation 2 while Piciformes, Accipitriformes and Passeriformes, exhibit comparatively higher levels of integration in situation 3 than in situation 2. Passeriformes, Piciformes and Accipitriformes are among the clades that include the highest range of beak shapes whereas Psittaciformes do not include very disparate beak shapes in comparison (Fig. 2, Extended Data Figs. 2 & 3). For instance, Passeriformes have both extreme brachyrostral (e.g., *Paradoxornis*) and extreme longirostral taxa (e.g., *Epimachus*). Similarly, Eucavitaves, a clade encompassing the orders Piciformes (toucans, woodpeckers and akin), Coraciiformes (kingfishers, rollers and akin), Bucerotiformes (hornbills, hoopoes and woodhoopoes) and Trogoniformes (trogons), exhibits much higher cranial integration in situation 3 than any of its constituent clades (SI. Figs 5 & 6, Supplementary Data 3), which does not happen in situation 2 (Fig. 4, Table 1). Similarly, all non-passerines taken together have much higher levels of covariation than any of their constituent orders (SI. Figs 5 & 6, Supplementary Data 3). Both Eucavitaves and Passeriformes taken together exhibit much larger range of beak shapes than any of its constituent clades.

Therefore, on the light of these results, we interpret that integration measures in situation 3 are largely controlled by the disparity of localized variation in the beak region in our sample. Furthermore, we consider biologically unlikely that the changes in strength of covariation between the same clades in situation 2 and situation 3 are only due to differences in orientation and relative size of beak and skull blocks (i.e., the information which is lost when superimposing separately beak and skull landmarks, as in situation 2). We therefore interpret the differences in cranial integration between situation 2 and situation 3 as likely arising from a spread of local variation from the beak to the rest of the skull by GPA, seriously overestimating integration in clades where beak variation is high. In situation 2, however, local variation in the beak is not spread to the skull block because GPA are conducted separately, so measures of integration are not laden with artefactual variation, confirming previous results [9]. We therefore echoe Cardini's[9] conclusions in considering crucial to understand how variation might be distributed in the sample before conducting analysis of integration/modularity. Although these are some of the several tools that can help with identifying and copying with this issue, ideal solutions are still unexplored and underdeveloped. Developing methods able to cope with these issues while still being consistent with Procrustes distances approaches, although far from the scope of this study, might likely be a fertile area for future research in geometric morphometrics.

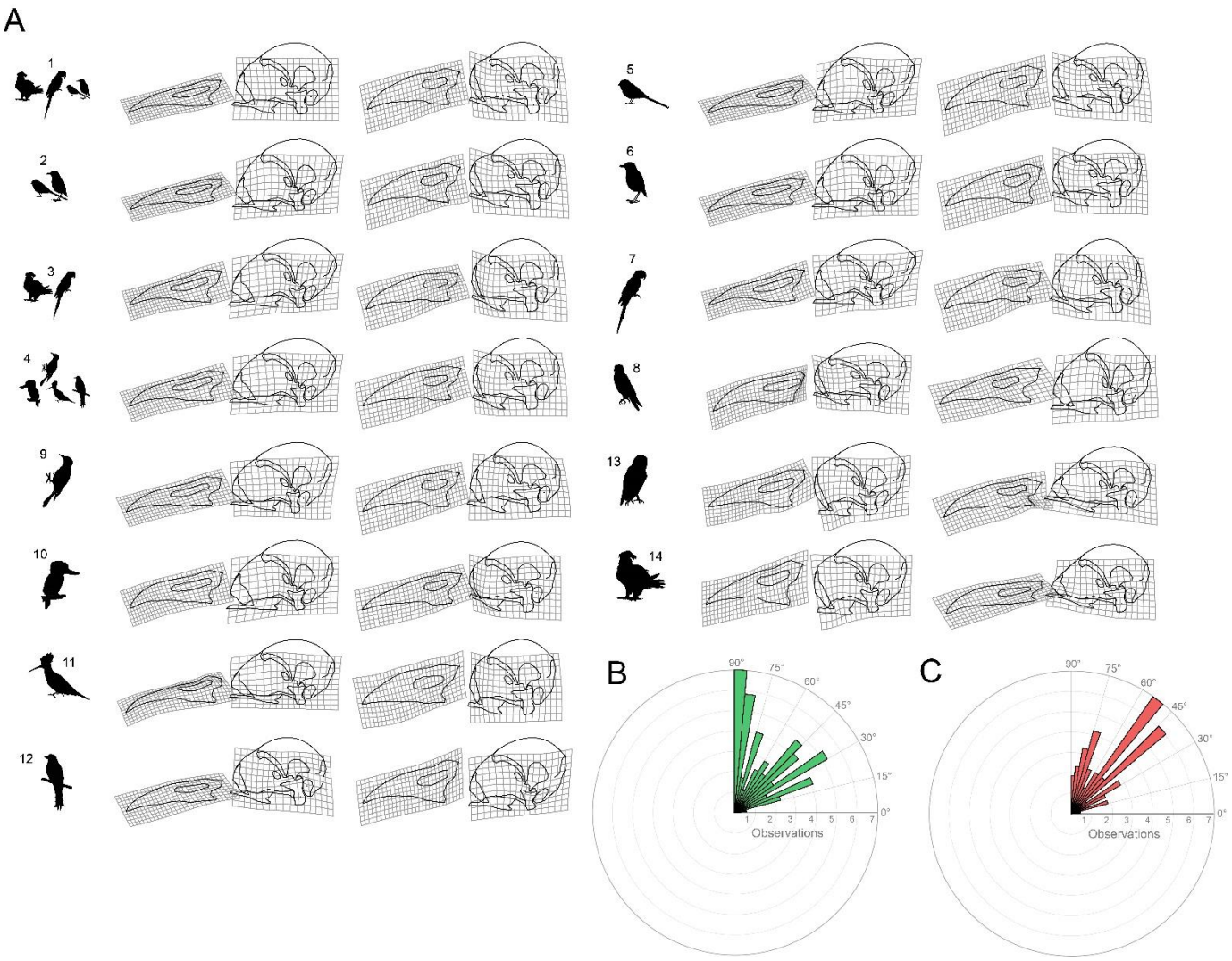

SI. Figure 1. Shape differences associated with the first pair of PLS vectors (PLS1) for the beak block and the skull block for the main lineages of landbirds. Polar histograms summarizing angle comparisons between the PLS1 vectors for the beak (B) and skull (C) blocks. As orientation of PLS1 vectors is arbitrary, the maximum possible angle between PLS1 vectors is 90°. * indicates single angular comparison of the PLS1 vectors of Passerida excluding DF and HH.

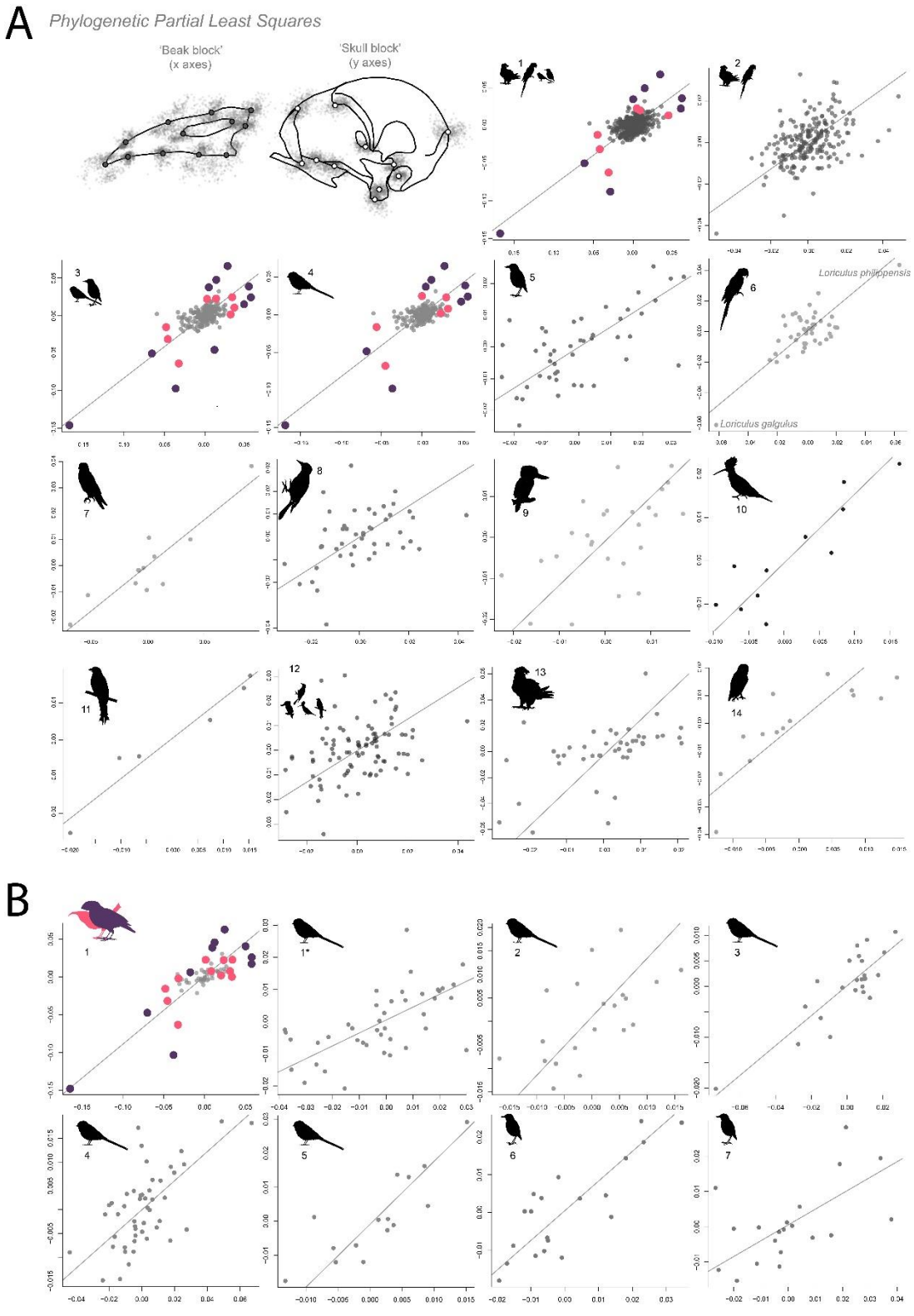

SI. Figure 2. PLS1 plots for the Within One Configuration Phylogenetic Partial Least Squares Analyses using the time tree (situation 1, see SI. Extended Methods) per clade division (numbers correspondence in Table 1.). Y axes, PLS1 scores beak block; X axes, PLS1 scores skull block. A) Major landbird lineages, B) Major lineages of passerines.

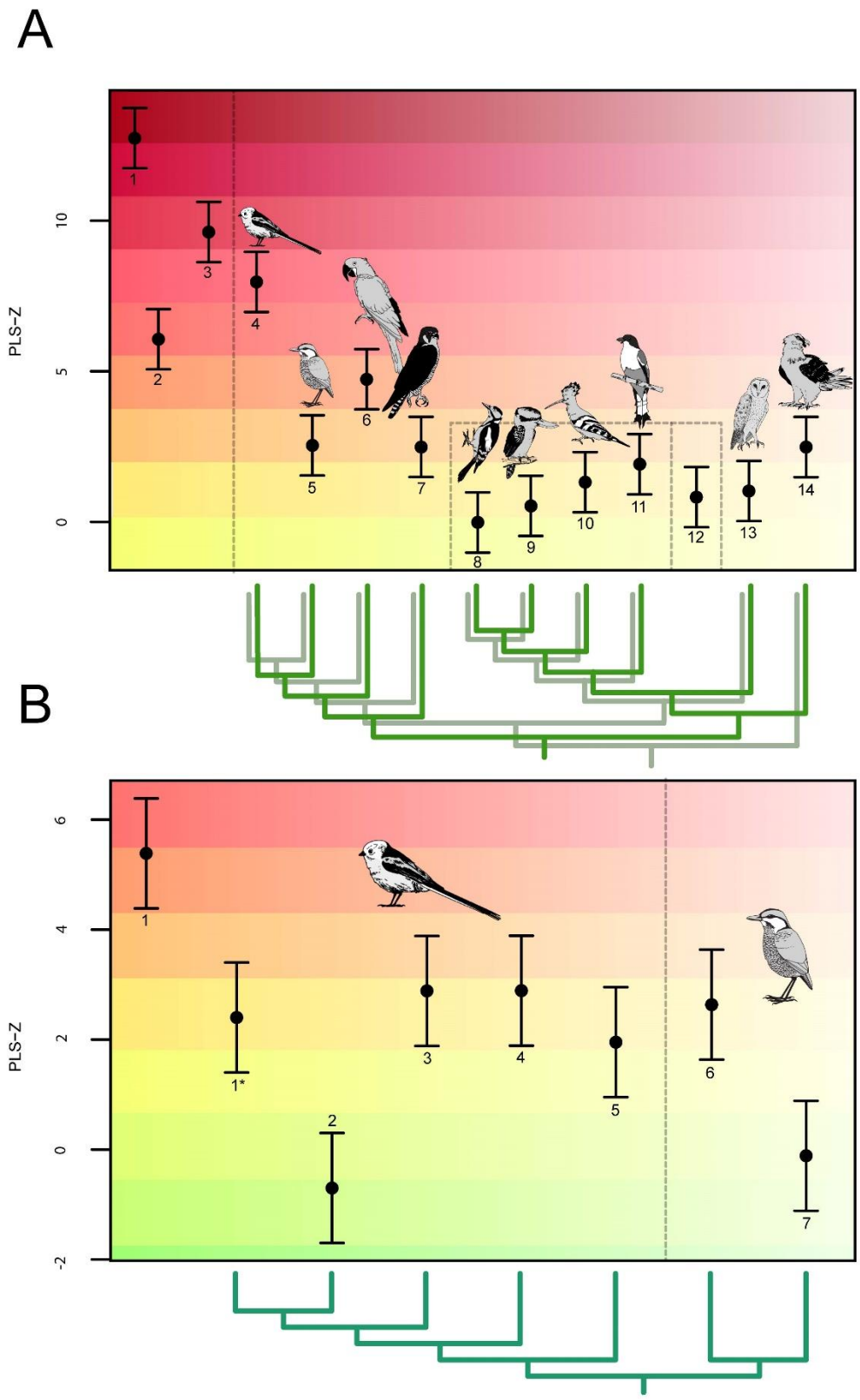

SI. Figure 3. Strength of evolutionary shape covariation between beak and skull. Z-scores are effects sizes calculated from the randomized distribution of *rpls* values from the phylogenetic PLS for each clade (situation 1). Cladograms portray the simplified phylogenetic relationships of the main lineages in our phylogeny (solid colour) as compared to other recently published phylogenetic hypothesis (Prum et al. 2015, transparent colour in A).

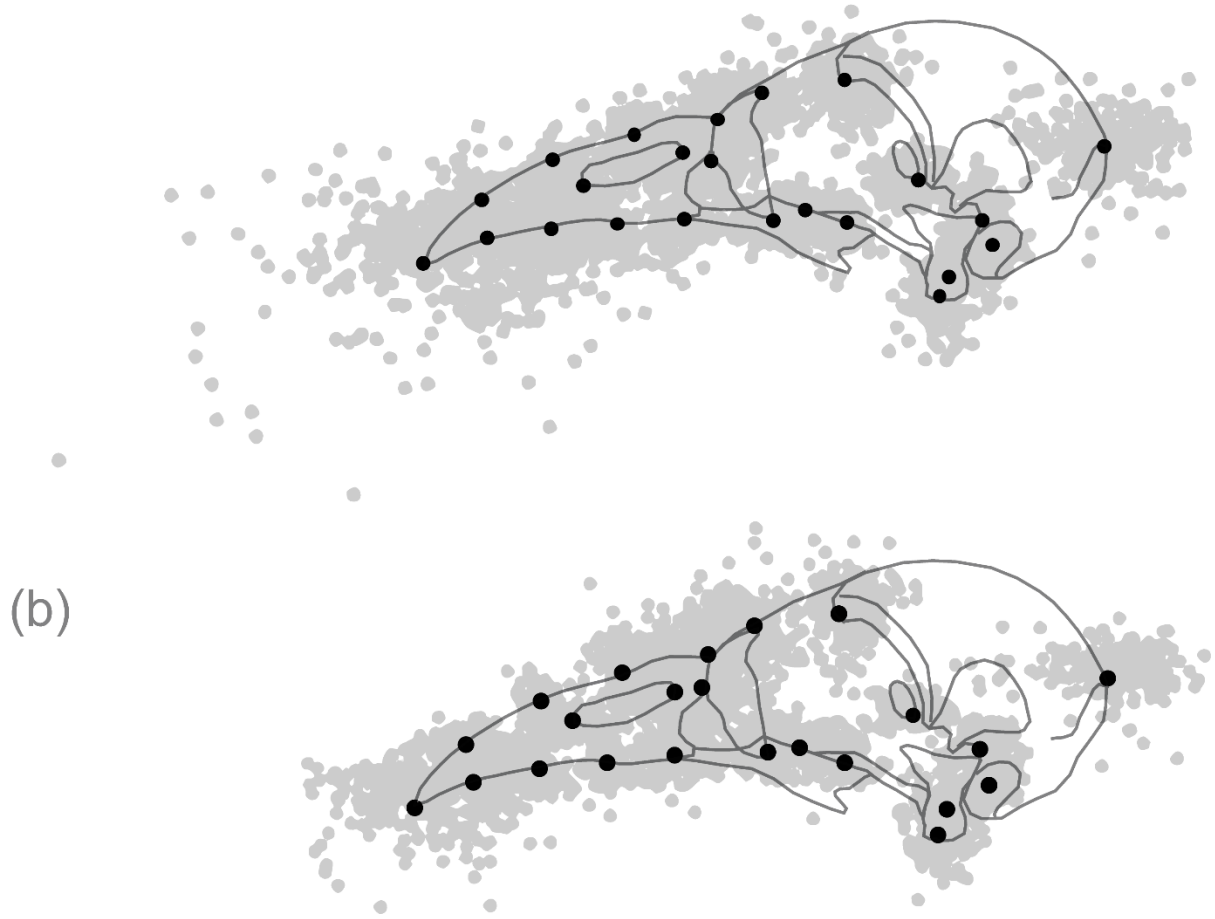

SI. Figure 4. Superimposed whole skull configurations for the 436 specimens (grey dots) and consensus configuration (black dots) using GRPS (resistant fit based superimposition) (A) and GPS (least squares-based superimposition) (B). GRPS reveals a great deal of variation in the beak region that GPS repartitions across the whole configuration. Outline diagrams were overlain using Adobe Illustrator to aid visual inspection of the plots.

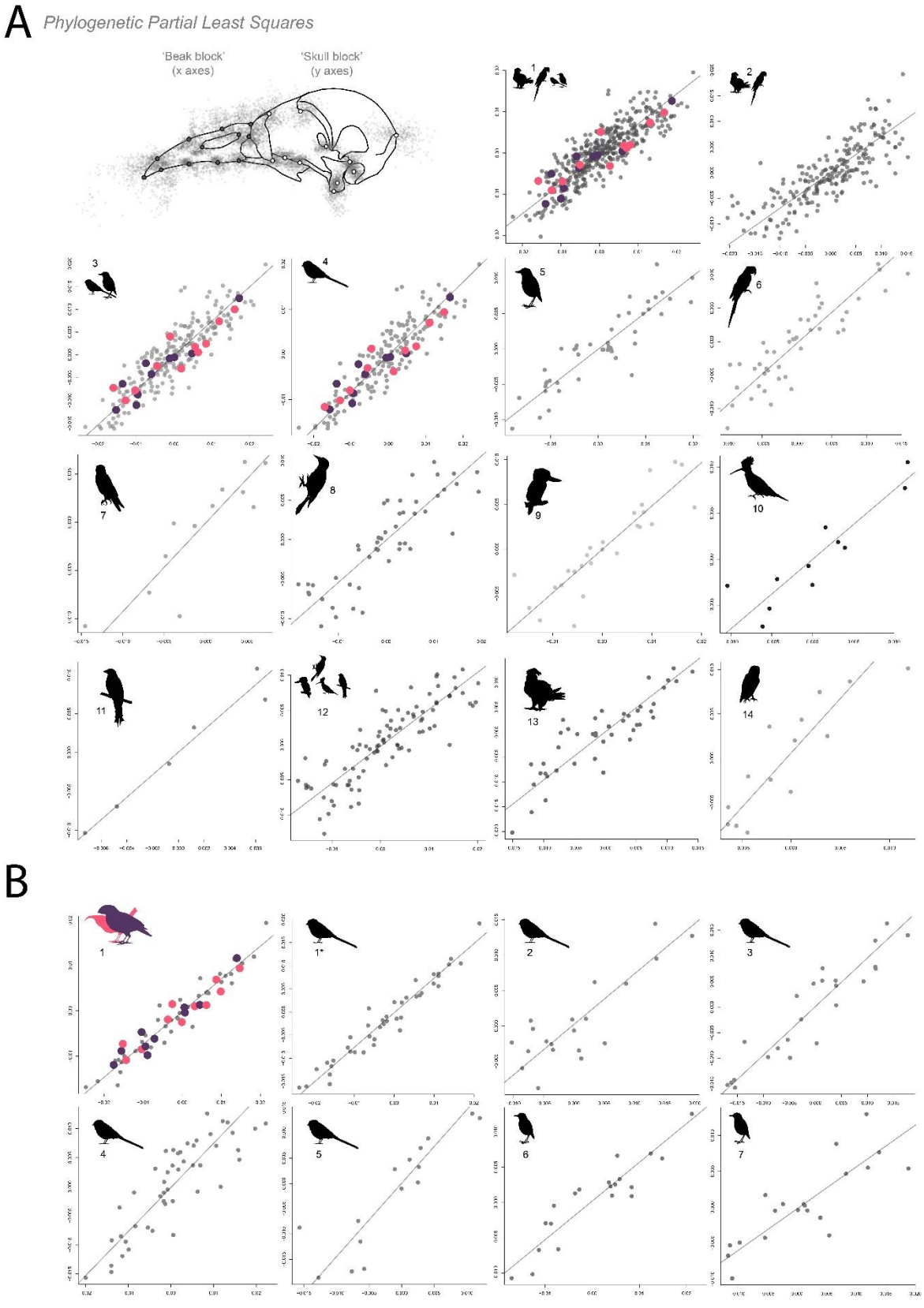

SI. Figure 5. PLS1 plots for the Two Blocks Phylogenetic Partial Least Squares Analyses using the rate-scaled phylogeny (situation 3, see SI. Extended Methods) per clade division (numbers correspondence in Table 1). Y axes, PLS1 scores beak block; X axes, PLS1 scores skull block. A) Major landbird lineages, B) Major lineages of passerines.

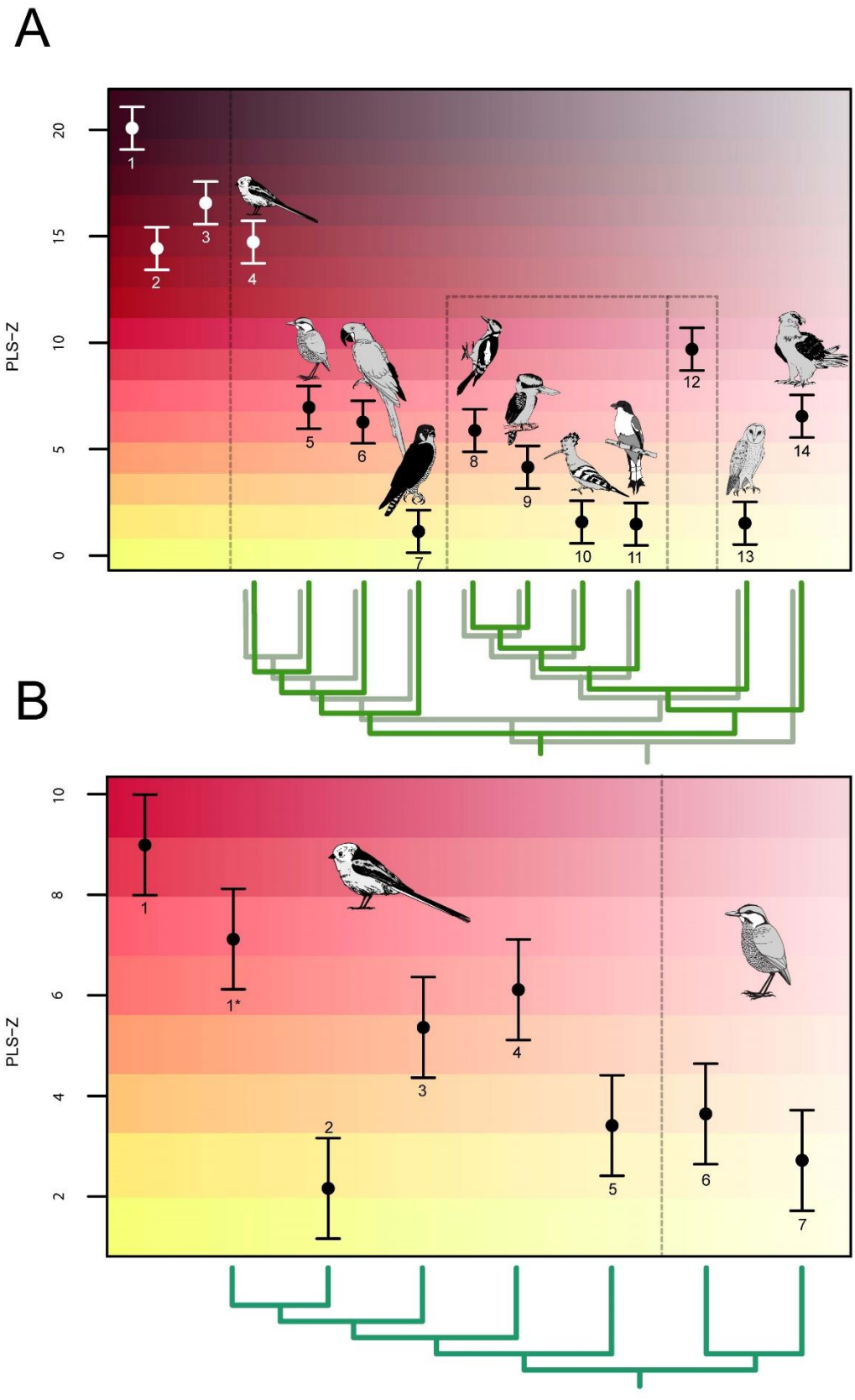

SI. Figure 6. Strength of evolutionary shape covariation between beak and skull. Z-scores are effects sizes calculated from the randomized distribution of *rpls* values from the phylogenetic PLS for each clade (situation 3). Cladograms portray the simplified phylogenetic relationships of the main lineages in our phylogeny (solid colour) as compared to other recently published phylogenetic hypothesis (Prum[10], transparent colour in A).

WHOLE SKULL

Branch shifts

Order	Families*	Genera	N	Fold increase	PP
ACCIPITRIFORMES	Accipitridae	*Lophaetus occipitalis*	1	6.66	0.99995
	Accipitridae	*Torgos tracheliotos*	1	13.84	0.7692
	Accipitridae	*Circus approximans*	1	5.55	0.99825
BUCEROTIFORMES	Bucerotidae, Upupidae, Phoeniculidae	*Buceros rhinoceros, Penelopides affinis, Aceros undulatus, Anthracoceros marchei, Ceratogymna atrata, Bycanistes bucinator, Tockus erythrorhynchus, Bucorvus abyssinicus, Phoeniculus purpureus, Rhinopomastus cyanomelas, Upupa epops*	11	28.32	0.86875
CORACIIFORMES	Alcedinidae	*Dacelo novaeguineae*	1	4.82	0.97835
PASSERIFORMES	Cotingidae (Tyrannida)	*Rupicola peruvianus*	1	6.47	1
	Thraupidae (Passerida)	*Coereba flaveola*	1	7.84	0.9995
	Nectariinidae (Passerida)	*Arachnothera magna*	1	4.25	0.9982
	Vangidae (Corvides)	*Falculea palliata*	1	10.12	0.9979
	Drepanidinae, Fringillidae (Passerida, HH)	*Vestiaria coccinea*	1	45.77	0.99245
	Timaliidae (Sylviida)	*Paradoxornis webbianus*	1	4.74	0.99095
	Alaudidae (Sylviida)	*Mirafra javanica*	1	3.32	0.972
	Malaconotidae (Corvides)	*Pityriasis gymnocephala*	1	2.53	0.9093
	Thraupidae (Passerida, GF)	*Geospiza conirostris*	1	70.22	0.9028
	Thraupidae (Passerida, GF)	*Geospiza magnirostris*	1	55.88	0.8914
	Zosteropidae (Sylviida)	*Zosterops flavifrons*	1	2.46	0.84475
	Tityridae (Tyrannida)	*Tityra semifasciata*	1	2.18	0.807
	Paradiseidae (Corvides)	*Epimachus fastuosus*	1	6.83	0.7266
PICIFORMES	Ramphastidae	*Ramphastos dicolorus, Pteroglossus viridis, Aulacorhynchus prasinus, Selenidera reinwardtii, Andigena laminirostris*	5	28.32	0.99995
PSITTACIFORMES	Psittacidae	*Micropsitta finschii*	1	6.09	0.9882
	Psittacidae	*Loriculus galgulus*	1	22.73	0.983
	Psittacidae	*Trichoglossus ornatus*	1	6.87	0.95165
STRIGIFORMES	Strigidae	*Bubo bubo*	1	7.16	0.99965

Node shifts

ACCIPITRIFORMES	Accipitridae	*Rostrhamus sociabilis, Ictinia plumbea*	2	2.13	0.82745
PASSERIFORMES	Furnariidae (Furnariida)	*Xenops minutus, Asthenes pyrrholeuca, Pseudocolaptes boissonneautii, Upucerthia jelskii, Lochmias nematura, Margarornis squamiger, Xiphocolaptes albicollis, Xiphorhynchus guttatus, Lepidocolaptes souleyetii, Dendrocincla fuliginosa*	10	1.62	0.95225
	Ploceidae, Estrildidae, Viduidae (Passerida)	*Ploceus baglafecht, Euplectes ardens, Dinemellia dinemelli, Pytilia melba, Parmoptila woodhousei, Estrilda melpoda, Vidua fischeri*	7	1.74	0.9519
	Drepanidinae, Fringillidae (Passerida, HH)	*Loxops coccineus, Pseudonestor xanthophrys, Hemignathus kauaiensis, Hemignathus lucidus, Hemignathus munroi, Palmeria dolei, Vestiaria coccinea, Himatione sanguinea, Telespiza ultima, Loxioides bailleui*	10	3.74	0.80185

SI. Table 1. Rate shifts for the whole skull configurations.

BEAK BLOCK

Branch shifts

Order	Families*	Genera	N	Fold increase	PP
ACCIPITRIFORMES	Accipitridae	*Necrosyrtes monachus*	1	12.99	0.86845
FALCONIFORMES	Falconidae	*Daptrius ater*	1	47.04	0.96145
	Falconidae	*Falco mexicanus, Falco biarmicus, Falco peregrinus, Microhierax caerulescens, Polihierax insignis, Polihierax semitorquatus, Caracara plancus, Caracara cheriway, Daptrius ater, Milvago chimango, Phalcoboenus carunculatus, Herpetotheres cachinnans*	12	4.51	0.8035
	Falconidae	*Caracara plancus, Caracara cheriway*	2	11.63	0.73
PASSERIFORMES	Cotingidae (Tyrannida)	*Rupicola peruvianus*	1	13.89	1
	Timaliidae (Sylviida)	*Paradoxornis webbianus*	1	11.93	0.99645
	Vangidae (Corvides)	*Falculea palliata*	1	10.12	0.9911
	Tityridae (Tyrannida)	*Tityra semifasciata*	1	5.41	0.94435
	Drepanidinae, Fringillidae (Passerida, HH)	*Vestiaria coccinea*	1	51.73	0.9264
	Remizidae, Paridae (Sylviida)	*Remiz pendulinus, Parus major*	2	11.12	0.8938
	Thraupidae (Passerida, HH)	*Geospiza magnirostris*	1	81.64	0.84535
	Malaconotidae (Corvides)	*Pityriasis gymnocephala*	1	4.91	0.77665
	Nectariinidae (Passerida)	*Arachnothera magna*	1	2.94	0.71905
PICIFORMES	Ramphastidae	*Ramphastos dicolorus, Pteroglossus viridis, Aulacorhynchus prasinus, Selenidera reinwardtii, Andigena laminirostris*	5	12.49	0.8838
	Semnornithidae	*Semnornis ramphastinus*	1	4.33	0.83685
PSITTACIFORMES	Psittacidae	*Loriculus galgulus*	1	11.73	0.757
	Psittacidae	*Enicognathus leptorhynchus*	1	4.12	0.7229
Node shifts					
ACCIPITRIFORMES	Accipitridae	*Rostrhamus sociabilis, Ictinia plumbea*	2	3.57	0.91645
PASSERIFORMES	Monarchidae, Paradiseidae, Rhipiduridae, Struthideidae, Corcoracidae (Corvides)	*Semioptera wallacii, Paradisaea rubra, Epimachus fastuosus, Myiagra vanikorensis, Rhipidura rufiventris, Struthidea cinerea, Corcorax melanorhamphos*	7	2.22	0.89565
	Ploceidae, Estrildidae, Viduidae (Passerida)	*Ploceus baglafecht, Euplectes ardens, Dinemellia dinemelli, Pytilia melba, Parmoptila woodhousei, Estrilda melpoda, Vidua fischeri*	7	3.66	0.7662

SI. Table 2. Rate shifts for the beak block.

SKULL BLOCK					
Branch shifts					
Order	**Families***	**Genera**	**N**	**Fold increase**	**PP**
ACCIPITRIFORMES	Accipitridae	*Lophaetus occipitalis*	1	9.55	0.99485
	Accipitridae	*Circus approximans*	1	6.08	0.9888
	Accipitridae	*Torgos tracheliotos*	1	17.63	0.86735
CORACIIFORMES	Alcedinidae	*Halcyon smyrnensis*	1	4.71	0.8169
FALCONIFORMES	Falconidae	*Caracara cheriway*	1	4.49	0.7646
PASSERIFORMES	Thraupidae (Passerida)	*Coereba flaveola*	1	4.85	0.9864
	Paradiseidae (Corvides)	*Epimachus fastuosus*	1	3.82	0.96425
PICIFORMES	Megalaimidae	*Psilopogon pyrolophus*	1	6.32	0.9192
	Psittaciformes	All Psittaciformes			
PSITTACIFORMES			45	9.29	0.99925
	Psittacidae	*Trichoglossus ornatus*	1	10.90	0.9759
	Psittacidae	*Loriculus galgulus*	1	22.21	0.97035
	Psittacidae	*Chalcopsitta atra*	1	5.18	0.88745
STRIGIFORMES	Strigidae	*Bubo bubo*	1	9.08	0.998
	Strigidae	*Asio otus*	1	5.78	0.8974
Node shifts					
PASSERIFORMES	Passeri	All Passeri	178	0.41	0.8851
	Emberizidae (Passerida, GF)	*Platyspiza crassirostris, Pinaroloxias inornata, Camarhynchus pallidus, Geospiza scandens, Geospiza difficilis, Geospiza conirostris, Geospiza fuliginosa, Geospiza magnirostris, Certhidea olivacea*	9	6.19	0.8701
	Drepanididae (Passerida, HH)	*Loxops coccineus, Pseudonestor xanthophrys*	2	11.45	0.782
	Drepanididae (Passerida, HH)	*Loxops coccineus, Pseudonestor xanthophrys, Hemignathus kauaiensis, Hemignathus lucidus, Hemignathus munroi, Palmeria dolei, Vestiaria coccinea, Himatione sanguinea, Telespiza ultima, Loxioides bailleui*	10	2.72	0.75885

SI.Table 3. Rate shifts for the skull block.

Literature cited

1 Cooney, C. R. *et al.* Mega-evolutionary dynamics of the adaptive radiation of birds. *Nature* **542**, 344-347 (2017).

2 Tobias, J. A. *et al.* Species coexistence and the dynamics of phenotypic evolution in adaptive radiation. *Nature* **506**, 359 (2014).

3 Navalón, G., Bright, J. A., Marugán-Lobón, J. & Rayfield, E. J. The evolutionary relationship between beak shape, mechanical advantage, and feeding ecology in modern birds. *Evolution* (2018).

4 Zelditch, M. L., Ye, J., Mitchell, J. S. & Swiderski, D. L. Rare ecomorphological convergence on a complex adaptive landscape: body size and diet mediate evolution of jaw shape in squirrels (Sciuridae). *Evolution* **71**, 633-649 (2017).

5 Adams, D. C. & Collyer, M. L. Multivariate phylogenetic comparative methods: evaluations, comparisons, and recommendations. *Systematic biology* **67**, 14-31 (2017).

6 Uyeda, J. C., Caetano, D. S. & Pennell, M. W. Comparative analysis of principal components can be misleading. *Systematic Biology* **64**, 677-689 (2015).

7 Torcida, S., Perez, S. I. & Gonzalez, P. N. An integrated approach for landmark-based resistant shape analysis in 3D. *Evolutionary Biology* **41**, 351-366 (2014).
8 Siegel, A. F. & Benson, R. H. A robust comparison of biological shapes. *Biometrics*, 341-350 (1982).
9 Cardini, A. Integration and modularity in Procrustes shape data: is there a risk of spurious results? *Evolutionary Biology*, 1-16 (2018).
10 Prum, R. O. *et al.* A comprehensive phylogeny of birds (Aves) using targeted next-generation DNA sequencing. *Nature* (2015).